

Static, modal and dynamic behaviour of a stress ribbon footbridge: Experimental and computational results

Castaño, Javier¹; Cosido, Óscar²; Pereda, José³; Cacho-Pérez, Mariano³; Lorenzana, Antolín³

ABSTRACT

Response for the static, modal and dynamic problem corresponding to a stress ribbon footbridge is studied. The equilibrium equations describing the problem are coupled nonlinear differential equations which are numerically solved using the finite element method. The objective of this work is to present a proper computational model for such a structure and to check its applicability in predicting not only the static behaviour but also modal parameters and estimate its dynamic response. As the footbridge is continuously monitored, it has been possible to measure the sag and to identify natural modes. This experimental data has been used for updating the finite element model.

Keywords: finite element method, non-linear analysis, experimental techniques, model updating.

1. INTRODUCTION

Cables are common structural members in civil engineering. Although in most of the cases cables are working together with other structural members (beams, plates ...), in the application studied in this paper (stress ribbon footbridge) cables lead (together with the abutments) the structural strength and stability. The simple idea of installing ropes and wooden slabs for crossing a river has evolved in modern bridge designs like the ones of U. Finsterwalder in mid-20th century followed by J. Strasky, among others. Most of the stress ribbon footbridges are built in reinforced concrete using post-stressing techniques. With that typology, the concrete deck contributes with mass and transversal stability but the active tendons are the responsible for the static and dynamic behaviour. Other building alternative is to place precast concrete slabs over the main cables or plates, once pretensioned properly. In the footbridge under study (see figure 1), the plate is 85 m long and is made of steel, being its cross section 3.6 m wide and 30 mm thick.

Despite the wide use of catenary-like structures, its analytical or computational modelling is not straight forward. The main drawback for its study is the geometrical non-linearity associated to the large displacements that appear, so the equilibrium must be established on the deformed configuration. Under certain simplifications (uniform mass distribution, inextensibility ...) there is analytical solution for determining the deformed shape (catenary) and also the natural frequencies and the modal shapes. Note that the solution depends on internal parameters as the weight or the

¹ Mechanical Engineering Division, CARTIF Research Center (Spain). javcas@cartif.es

² A.M. and Computational Techniques Dept., ETSIT, University of Cantabria (Spain). oscar.cosido@unican.es

³ EII/ITAP, University of Valladolid (Spain). pereda@eii.uva.es, cacho@eii.uva.es, ali@eii.uva.es (Corresponding author)

initial tension that cannot be easily identified once the structure is in use. Besides, real cases are affected by elongation due to the axial force, thermal expansion due to the temperature changes and in some cases unequal mass distribution along the structure. For these cases, the solution to the analytical formulation must be obtained by numerical techniques or using computational approaches based on the finite element method. In real applications, internal unknown parameters prevent initial analytical or numerical models to match with experimental results. Standard trial-and-error techniques must be used to estimate proper values of those parameters in a logical range so simulation response can be close to the real one.



Figure 1. Stress ribbon footbridge under study

The objective of this work is to present a proper finite element model for such a non-linear structure and to check its applicability in predicting not only the static behaviour but also the modal and dynamic ones. For that, two different models have been created, one using cable-type elements (1D) and other with shell-type elements (2D). Both models have been updated by numerical iterative methods employing data measured from the actual footbridge. Finally the accuracy of each method is evaluated.

2. MECHANICS OF A SUSPENDED CABLE

The mathematic expressions describing the mechanical behaviour (static and dynamic) of a suspended cable are an ensemble of non-linear coupled differential equations. These equations can only be analytically solved after linearization (Irvine's suspended cable linear theory [1]) and assuming certain simplifications otherwise the solution can only be obtained by numerical analysis.

For hanging plates, the behaviour in the vertical plane is similar considering the plate is working as a membrane. Additionally, transverse and torsional modes can appear. To evaluate these modes general shell theory [3] must be applied. The resulting equations are solved employing numerical

techniques which demand spatial discretization and interpolation in a similar way finite element methods do.

3. APPLICATION TO THE STRESS RIBBON FOOTBRIDGE

The Pedro Gómez Bosque footbridge case is analysed. This pedestrian bridge, sited in Valladolid (Spain), is a slender and lightweight steel stress ribbon structure built in 2011 with only one span of approximately 85 m that provides minimal impact on the surroundings. It mainly consists of a Corten steel sheet 94 m long, 3.6 m wide and only 30 mm thick, which is pretensioned and anchored to the two abutments, which are 2 m not on level. The complete steel sheet is fabricated by 8 m long plates welded. A number of 110 precast concrete slabs 5.2 m long, 0.75 m wide and 120 mm thick, lay on the steel sheet. The structure is completed by rubber pavement and stainless steel and glass handrail. All these structural and functional parts suppose around 23.6 kN/m. Initial pretension on the steel sheet was adjusted so the displacement in the middle were limited to $L/50$ which means 1.7 m.

3.1. Experimental

3.1.1. Static measurements

Surveying techniques combined with photogrammetry ones were used for determining the deformed shape. First, two pairs of reference points were chosen in the abutments. Then, 8 intermediate pairs of points were selected along the deck. Each pair of points is 2.4 m apart in the transversal direction of the deck. All the resulting 10 upstream points were aligned, and also all the downstream ones. Setting the base in the higher abutment, a total station (theodolite integrated with an electronic distance meter) was used to read, with the help of a direct reading optical rod, the distance and elevation of the remaining 9 pair of points. Three measurements rounds were made and mean values obtained. After the statistical analysis, and according to the accuracy of the instrumentation, the maximum error was estimated in 6 mm. Note that the footbridge is prone to oscillate and amplitudes around 10 mm are usual even though the technician using the rods moves carefully. Finally, mean values in each pair of points were used as the reference coordinates for the subsequent adjustment of the finite elements models. This procedure was carried out in two different days with ambient temperatures of 18 °C and 28 °C. Results are shown in figure 2.

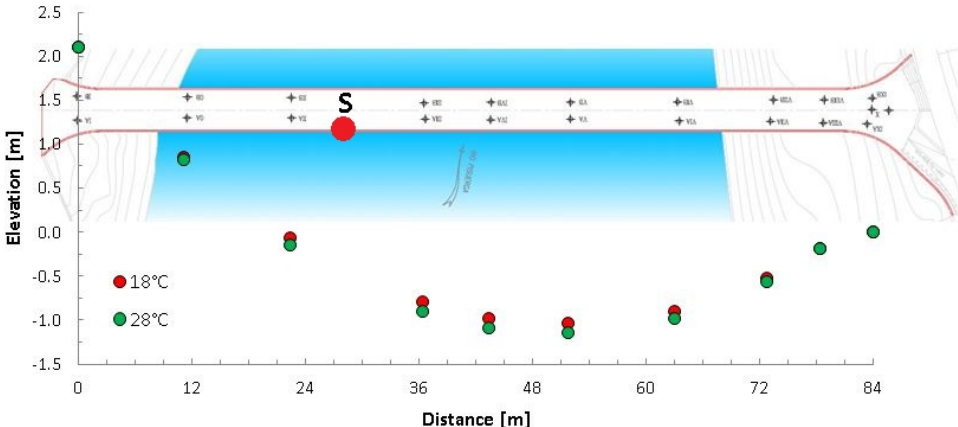


Figure 2. Measured elevations along the deck

Additionally to the topographic data, several photographs were taken and the corresponding 3D virtual model was built. Once adjusted using some reference points, the 3D model can be used (photogrammetry) to check distances and elevations of the selected pairs of points and to measure in any other point.

3.1.2. Modal and dynamic measurements

Since this footbridge was monitored with several accelerometers, the recordings were used to perform an Operational Modal Analysis to determine its free vibration modes. Table 1 presents the seven natural frequencies identified by FFD and SSI techniques at 20 °C. Corresponding modes are shown in figure 4. The notation used is BZ-I for bending modes in the vertical XZ plane, BY-I for bending modes in the horizontal XY plane and TX-I for torsional modes around X axis. *i* is the number of antinodes of the corresponding mode. No longitudinal modes have been observed and horizontal bending modes observed are always coupled with the torsional ones.

Additionally a dynamic test was carried out using and electrodynamic shaker placed in point S (see figure 2). Adjusting different parameters, a sinusoidal vertical force $F(t) = 230 \cdot \sin(2 \cdot \pi \cdot 1.780 \cdot t) [N]$ was generated during 90 s, as shown in figure 3, being 1.780 Hz the frequency of the fourth vertical bending mode. Resulting vertical accelerations in the same point S ($x = 28$ m) were also registered.

Table 1. Experimental frequencies

$T_{ref} = 20^{\circ}C$	vertical $f_{V,i}$ (Hz)	transversal + torsional $f_{HT,i}$ (Hz)
mode 1	1.020 BZ-1	1.050 BY-1+TX-1
mode 2	0.868 BZ-2	1.530 BY-2+TX-2
mode 3	1.410 BZ-3	2.230 BY-3+TX-3
mode 4	1.780 BZ-4	

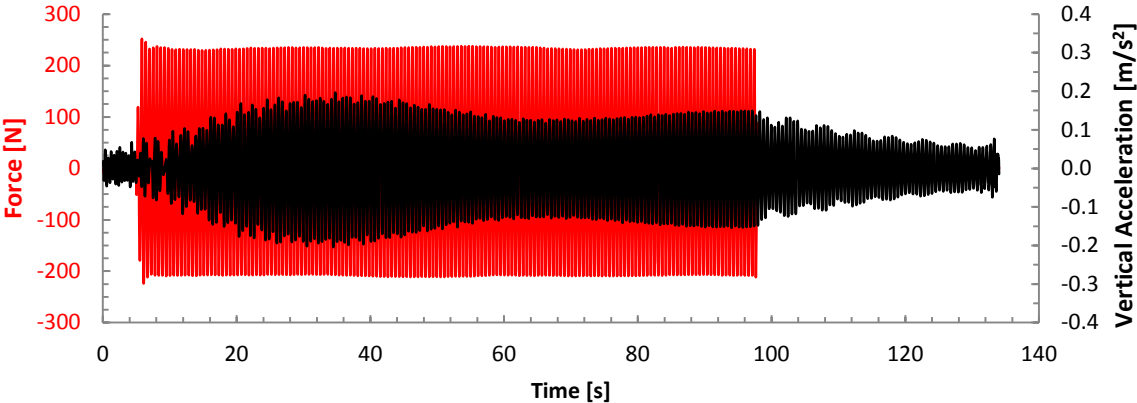


Figure 3. Dynamic test: Forced and free response of the footbridge

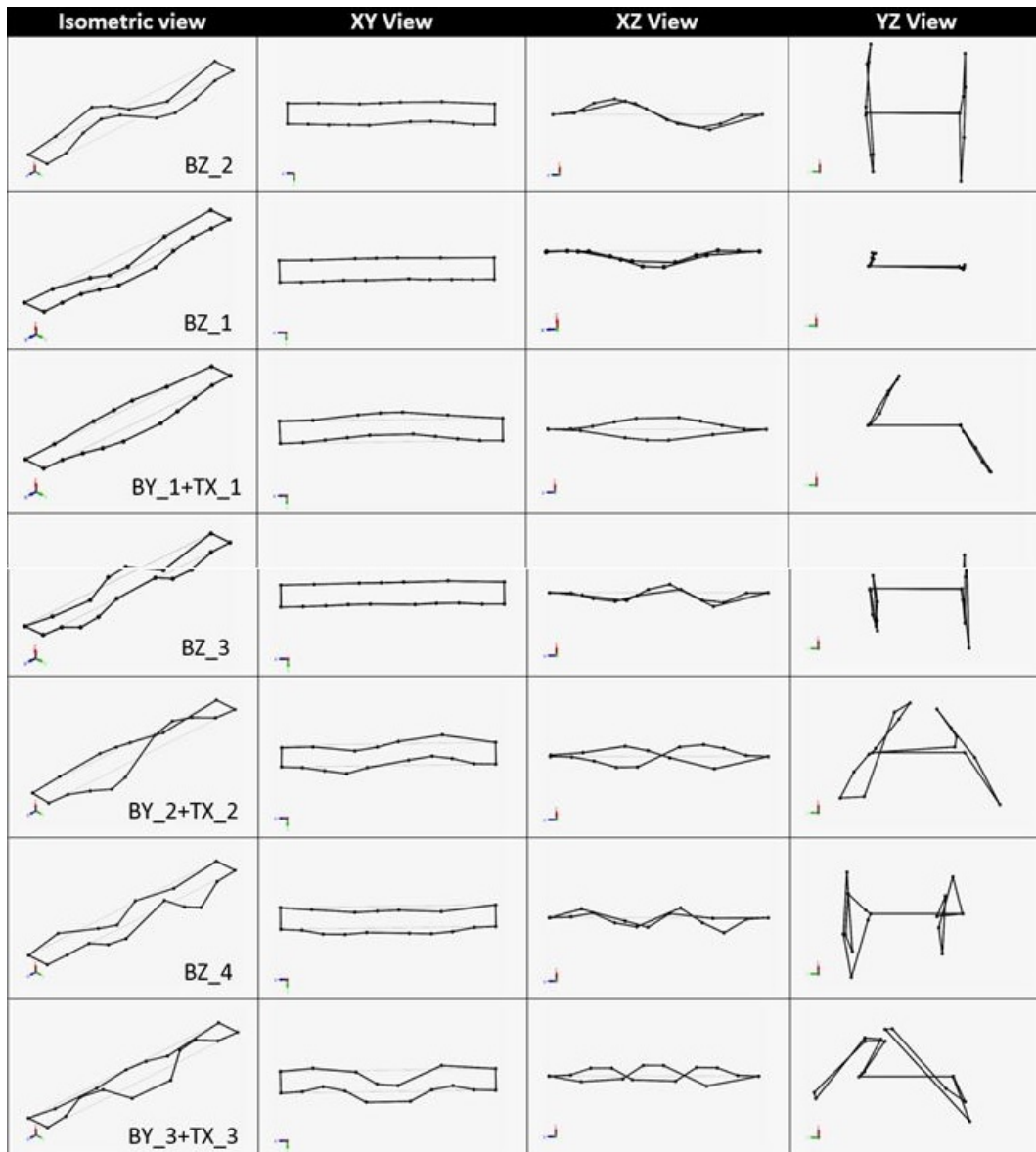


Figure 4. Experimental mode shapes for the first seven modes

3.2. Computational

3.2.1. FE Modelling and Model Updating

The computational part of this work has been done with the finite element software ANSYS® 15.0. Two footbridge models have been created. The first one is made of 200 cable-type elements (LINK180) while the other uses 2400 shell-type elements (SHELL181) instead.

The lack of knowledge of certain internal parameters of the footbridge (like the precise position of the extremes or the elastic properties of the structure as a whole) makes impossible to build a model able to reproduce the actual footbridge's behaviour using only data from the initial design project. Part of this work is setting those parameters to match the experimental static deformed shapes (measured at 18°C and 28°C) and the free vibration modes (measured at 20°C).

The parametric model updating has been carried out by numerical iterative techniques using the ANSYS® DesignXplorer application. The parameters selected for updating were the axial and torsional rigidity, the distributed load, the initial length and the horizontal distance between supports.

3.2.2. Static and modal results

After several goes, considering together the static and modal available data, the values of the governing parameters were fixed according with table 2. The maximum displacements obtained in each updated model are presented in Table 3. The matching achieved between each model and the experimental data is shown in figure 5.

Table 2. Updated parameter's values

Initial length	82.363	<i>m</i>
Horizontal distance	82.280	<i>m</i>
Mass distribution	2417	<i>kg/m</i>
Axial stiffness	4.573E8	<i>N/m</i>
Torsional stiffness	1.982E9	<i>N-m/rad</i>

Table 3. Comparison of sags for different temperatures

Temperature °C	EXPERIMENTAL		FINITE ELEMENT ANALYSIS			
	δ_{max} <i>m</i>	Cable-type model		Shell-type model		
		δ_{max} <i>m</i>	Error %	δ_{max} <i>m</i>	Error %	
18	1.993	1.956	1.89	1.958	1.78	
28	2.107	2.054	2.49	2.057	2.37	

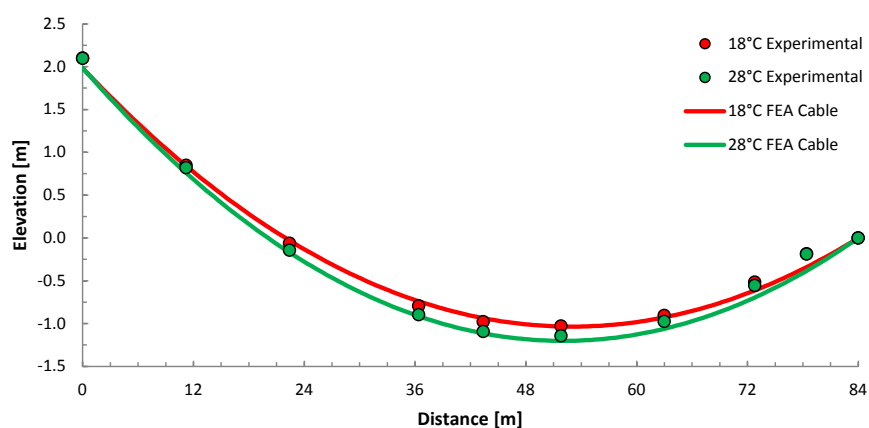


Figure 5. Static deformed shapes for different temperatures

Table 4 shows the natural frequencies for each updated model with a temperature of 20°C. The modal shapes of the cable model and the shell model are shown in figures 6 and 7.

Table 4. Comparison of natural frequencies at 20 °C

Mode	EXPERIMENTAL		FINITE ELEMENT ANALYSIS		
	f_i Hz	Cable-type model		Shell-type model	
		f_i Hz	Error %	f_i Hz	Error %
BZ-2	0.868	0.867	0.11	0.876	0.92
BZ-1	1.020	1.063	4.20	1.071	4.95
BY-1+TX-1	1.050	-	-	1.168	11.20
BZ-3	1.410	1.425	1.08	1.432	1.58
BY-2+TX-2	1.530	-	-	1.475	3.58
BZ-4	1.780	1.736	2.47	1.758	1.24

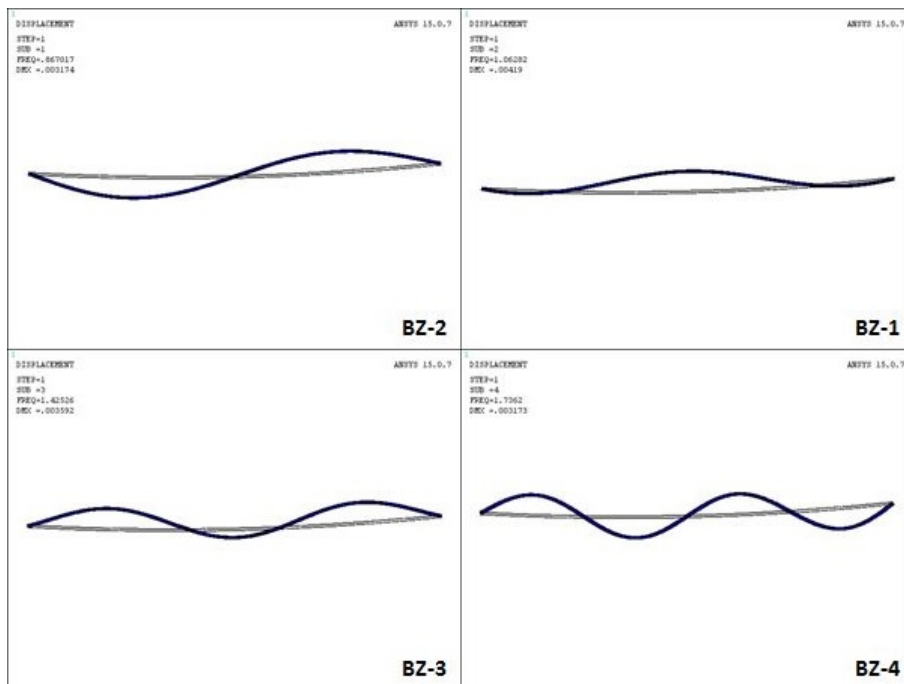


Figure 6. First four modal shapes of the cable FE model

3.2.3. Dynamic results

The structural damping has been introduced using the Rayleigh damping procedure. The damping coefficients alpha and beta have been set to achieve an approximate damping of 0.25% for all the considered modes. This damping ratio has been obtained adjusting the exponential free-decay curve in the structural response shown in figure 4 in the range 100 to 134 s.

In order to simulate the real measuring conditions, the force has been applied at the same point in the model and in the test. The force was a harmonic-type force with amplitude of 236 N and the frequency of the fourth mode of vertical bending that was applied during 100s. After that, the structure was left in free response for another 34 s. The experimental temperature was unknown, so the modal adjustment temperature was taken instead (20°C).

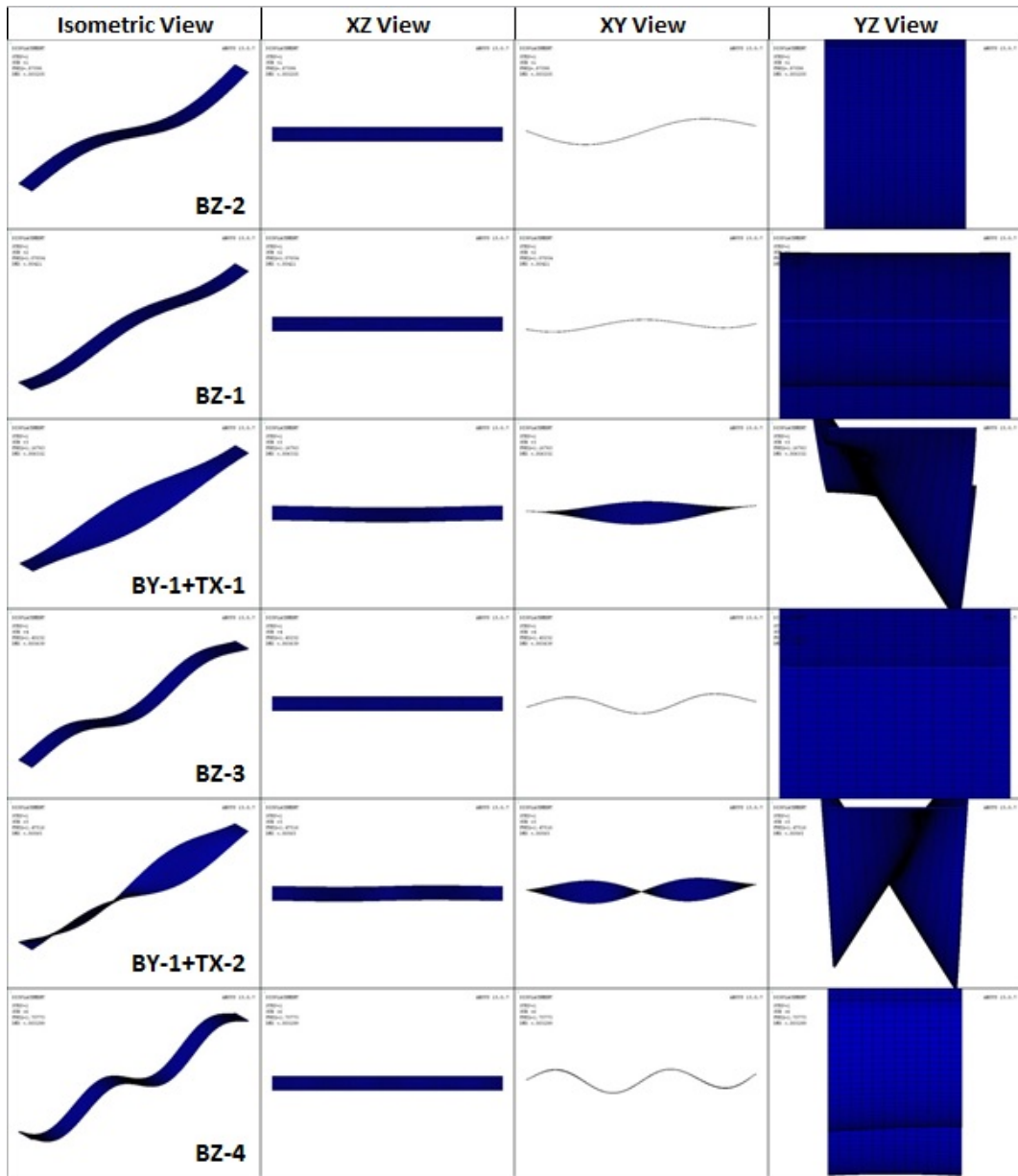


Figure 7. First six modal shapes of the shell FE model

3.2.4. Dynamic results

The structural damping has been introduced using the Rayleigh damping procedure. The damping coefficients alpha and beta have been set to achieve an approximate damping of 0.25% for all the considered modes. This damping ratio has been obtained adjusting the exponential free-decay curve in the structural response shown in figure 4 in the range 100 to 134 s.

In order to simulate the real measuring conditions, the force has been applied at the same point in the model and in the test. The force was a harmonic-type force with amplitude of 236 N and the frequency of the fourth mode of vertical bending that was applied during 100 s. After that, the

structure was left in free response for another 34 s. The experimental temperature was unknown, so the modal adjustment temperature was taken instead (20°C).

The figures 8 and 9 show the vertical acceleration data at the force application point. It can be noted that the response in both models match the one of a system at resonance, but the experimental data doesn't. This happens because the shaker doesn't have the accuracy of the numerical models, being unable to keep the actual structure at resonance. To make the models show this behaviour the force's frequency was modified with a small divert from the resonance (<1%).

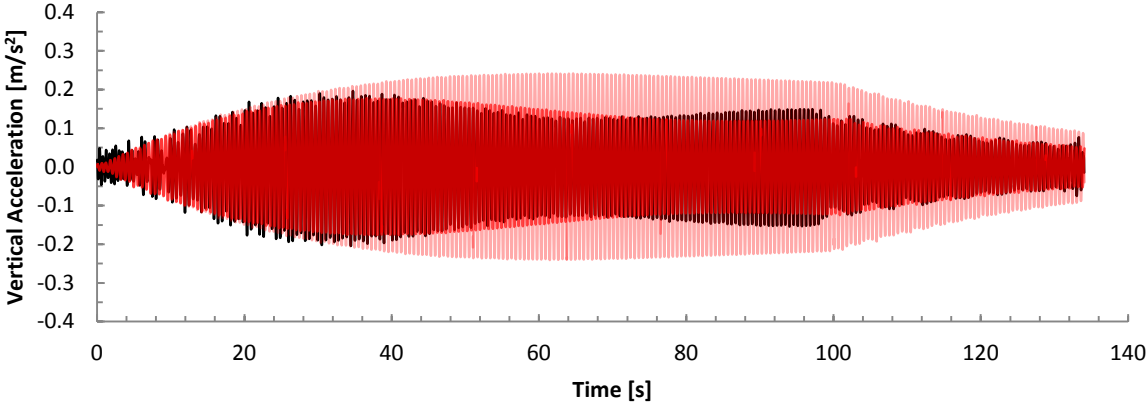


Figure 8. Dynamic response (Cable-type model): **black** - experimental; **pale red** - FEA at resonance; **red** - FEA slightly out of resonance

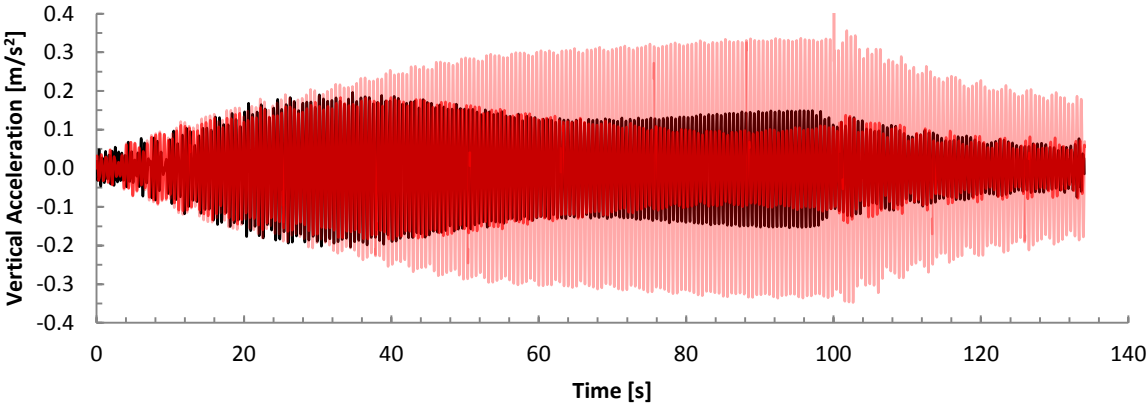


Figure 9. Dynamic response (Shell-type model): **black** - experimental; **pale red** - FEA at resonance; **red** - FEA slightly out of resonance

4. CONCLUSIONS

Cable and shell mathematical models have been developed to simulate the mechanical behaviour of a footbridge. Using the cable model, static and modal response in the vertical direction has been adjusted. But in order to incorporate the behaviour outside the vertical plane it is necessary to formulate the shell model. Once adjusted to static and modal experimental data, both models agree in the vertical direction. Shell model is additionally able to adjust the coupled modes that appear in the horizontal bending and torsional directions.

Using the updated models, the dynamic response matches with the loading test, showing the applicability of the numerical approach to study geometrical non-linear pedestrian structures.

ACKNOWLEDGEMENTS

This work has been partially funded by the Spanish Government Research Program with the Grant BIA2011-28493.

REFERENCES

- [1] Strasky, J. (2005). Stress ribbon and cable-supported pedestrian bridges. Thomas Telford Publishing.
- [2] Irvine, H.M. (1981). Cable Structures. The MIT Press.
- [3] Timoshenko, S., Woinowsky-Krieger, S. (1959). Theory of plates and shells. McGraw–Hill.
- [4] ANSYS® Mechanical APDL R15.0. Structural Analysis Guide. ANSYS, Inc.
- [5] Lepidi, M., Gattulli, V. (2012). Static and dynamic response of elastic suspended cables with thermal effects. *International Journal of Solids and Structures*, 49(9), 1103-1116.
- [6] Luongo, A., Zulli, D (2012). Dynamic instability of inclined cables under combined wind flow and support motion. *Nonlinear Dynamics*, 67(1), 71–87.
- [7] Bouaanani, N., Ighouba, M. (2011). A novel scheme for large deflection analysis of suspended cables made of linear or nonlinear elastic materials. *Advances in Engineering Software*, 42(12), 1009–1019.
- [8] Sandovic, G., Juozapaitis, A., Kliukas, R. (2011). Simplified engineering method of suspension two-span pedestrian steel bridges with flexible and rigid cables under action of asymmetrical loads. *Baltic Journal of Road and Bridge Engineering*, 6(4), 267–273.